Characterization of liquid phase epitaxial GaAs for Blocked-Impurity-Band far-infrared detectors

B.L. Cardozo [a,b] L.A. Reichertz [c,b] J.W. Beeman [b]

E.E. Haller [a,b,*]

[a] *Department of Materials Science and Engineering, University of California Berkeley, Berkeley, California 94720, USA*

[b] *Materials Sciences Division, Lawrence Berkeley National Laboratory, Berkeley, California 94720, USA*

[c] *Department of Physics, University of California, Berkeley, California 94720, USA*

Abstract

GaAs Blocked-Impurity-Band (BIB) photoconductor detectors have the potential to become the most sensitive, low noise detectors in the far-infrared below 45.5 cm^{-1} (220 μm). We have studied the characteristics of liquid phase epitaxial GaAs films relevant to BIB production, including impurity band formation and the infrared absorption of the active section of the device. Knowledge of the far-infrared absorption spectrum as a function of donor concentration combined with variable temperature Hall effect and resistivity studies leads us to conclude that the optimal concentration for the absorbing layer of a GaAs BIB detector lies between 1×10^{15} and 6.7×10^{15} cm^{-3}. At these concentrations there is significant wavefunction overlap which in turn leads to absorption beyond the 1s ground to 2p bound excited

state transition of 35.5 cm^{-1} (282 μm). There still remains a gap between the upper edge of the donor band and the bottom of the conduction band, a necessity for proper BIB detector operation.

Key words: BIB, Gallium Arsenide, LPE, far-infrared detectors

PACS: 07.57.Kp, 85.60.Gz, 95.55.Sh

---

1 Introduction

The far-infrared region of the electromagnetic spectrum is of great interest to astronomers studying star formation and distant galaxies [1]. Strong atmospheric absorption and emission of far-infrared radiation prevent the study of cosmic far-infrared signals except from very high altitude or space based telescopes. This limitation places high demands on detectors, the associated electronics, and the cryogenic systems. The two major types of detectors used for far-infrared observations, photoconductors and thermal detectors, or bolometers, have to be adapted for use under these conditions.

Detection in the case of a bolometer occurs when far-infrared photons are absorbed by a material and convert their energy to phonons, thus raising the temperature of the system. The temperature increase is converted to an electrical signal by a transducer such as a semiconductor thermistor. Bolometers detect all absorbed radiation and thus have very wide spectral response. Therefore complex filters are used to select the spectral band of interest. Bolometers are highly linear devices for moderate incident photon fluxes. Their use in space-

* Corresponding author. Tel.: 510-486-5294; fax: 510-486-5530.
Email address: EEHaller@lbl.gov (E.E. Haller).

borne telescopes is complicated, however, by three major factors. First, for comparable noise equivalent power (NEP), a figure of merit defined as the incident power necessary to achieve a signal to noise ratio of one for a bandwidth of 1 Hz, bolometers must be operated at temperatures significantly lower than photoconductive devices. Second, semiconductor bolometers have a narrow dynamic range with respect to incident photon power and their responsivity (output voltage divided by input power) will change under varying background conditions. Third, the integration of bolometers and their readout electronics into large arrays is still an unsolved problem due to the complex assembly of each detector pixel and the lack of low noise multiplexed readout electronics. These three factors make the incorporation of semiconductor bolometers onto space telescopes very challenging both technically and economically. Research and development efforts directed at superconducting transition edge bolometers may eventually change this situation, at least in regard to array fabrication [2].

Response in a photoconductor based detector is due to the excitation of an electron (hole) from the ground state to a conduction (valence) band state by absorption of a photon. Photoexcited electrons or holes that become conducting will drift under an applied electric field. This current comprises the response signal of the photoconductor. To reach a certain NEP, photoconductors do not require the same extreme cooling as bolometers because there exists an activation energy for conduction. Use of photoconductors therefore involves much simpler cooling hardware which greatly eases the design of far-infrared telescopes operated in space. Photoconductor detectors are better suited for low background conditions than thermal detectors because they can be teamed with cold integrating amplifiers to increase sensitivity. Further-

more, in contrast to bolometers, many photoconductor detectors can easily be made into large arrays. Photoconductors, however, are only usable over a limited spectral range which is determined by the semiconductor bandgap or the impurity ionization energy.

Far-infrared extrinsic photoconductors operate based on the optical excitation of electrons (holes) bound to impurity states within the semiconductor host [3]. The spectral onset of such a detector is given by the ionization energy of an impurity bound carrier. Holes bound to shallow acceptors in Ge have ionization energies of approximately 11 meV, equivalent to 88.5 cm^{-1} (113 μm) [4]. Detectors based on the p-type doped Ge system have among the longest wavelength response of any standard photoconductor in wide use.

The operational spectral range of Ge:Ga photoconductor detectors has been extended beyond this limit by the application of a uniaxial stress [5]. Uniaxial stressing of germanium has the effect of lifting the four-fold degeneracy within the valence band and creating two doubly degenerate bands [6]. In the high stress limit, the splitting reduces the shallow acceptor binding energy from 11 to approximately 6 meV. This decreases the onset of photoconductivity to approximately 45.5 cm^{-1} (220 μm), currently the lowest energy that can be detected by a photoconductor-based detector. The complexity of the mechanical rig required to apply high stress limits the size of an array of stressed Ge:Ga photoconductor detectors. A 2x25 stressed Ge:Ga array is used by the Multiband Imaging Photometer (MIPS) [7], an instrument onboard the Space Infrared Telescope Facility (SIRTF, recently renamed Spitzer Telescope) [8] and a 16x25 array is being constructed for the Herschel telescope [9].

GaAs Blocked-impurity band (BIB) devices are a class of infrared detectors

being developed to answer the demand for long wavelength (< 45.5 cm^{-1} or > 220 μm) photoconductor based sensors. The BIB device is a modification of a bulk photoconductor. It consists of a doped absorbing semiconductor layer in series with a thin high purity layer [10]. The high purity layer blocks dark current associated with hopping and impurity band conduction in the doped layer. This allows for an increase in the active region doping concentration compared to a standard photoconductor, in which the concentration is limited to lower values by the onset of hopping conduction. The increased dopant concentration of the absorbing layer in a BIB detector compared to a standard bulk photoconductor greatly enhances the linear optical absorption coefficient α of the device. This leads to an increased quantum efficiency (number of photoexcited carriers generated per incident photon) meaning that a smaller volume of material will yield equivalent photon absorption. The reduced detector volume makes the BIB detector less susceptible to interactions with high energy cosmic rays.

As will be shown, BIB devices have the potential to offer response at very long wavelengths, where currently only bolometers can be used, without sacrificing the high sensitivity and operating temperatures of standard photoconductor detectors. Arrays of BIB detectors have been realized using doped silicon for detection at higher energies (≥ 333 cm^{-1} or 30 μm) [11–13]. Si BIB detectors, currently onboard the Spitzer Telescope [7], are used to detect radiation near 417 cm^{-1} (24 μm). They operate at a relatively easily obtainable temperature of 1.5 K. BIB detectors made from GaAs are expected to operate according to the general model developed for BIB detectors but, because of the much reduced dopant binding energy, at correspondingly longer wavelength and lower temperatures. They should be able to detect photons with wavelengths ex-

ceeding 300 μm. In this study we have determined, approximately, the optimal shallow donor density for the active region of the GaAs BIB detector based on far-infrared absorption and variable temperature Hall effect measurements of n-type GaAs Liquid Phase Epitaxial films.

2 BIB Detector Theory

The band diagrams for a BIB detector with no external bias (a), and under reverse bias (b), are shown in Figure 1.

[Fig. 1 about here.]

At low temperature (< 2 K), most electrons will be frozen out onto donor impurity sites. Free electrons generated by photons absorbed within the depletion region will be collected at the positively biased contact. The ionized donor charge state travels to the negative contact. The combined motion of the positive donor state and the electron results in a unity photoconductive gain. In contrast to the gain distribution in a standard photoconductor, unity gain leads to lower noise. The electrons bound within the impurity band cannot conduct through the high-purity blocking layer, since the blocking layer interrupts the conduction path for dark current as long as the impurity band does not overlap with the conduction band.

The depletion region width of an n-type BIB detector is given by Equation 1

$$w = \sqrt{\frac{2\epsilon\epsilon_{\mathrm{o}}(V_{\mathrm{a}} - V_{\mathrm{bi}})}{eN_{\mathrm{A}}} + b^2} - b \tag{1}$$

Here ϵ is the relative dielectric constant, $V_{\rm a}$ is the applied bias, $V_{\rm bi}$ is the built in bias, e is the electron charge, $N_{\rm A}$ is the compensating acceptor impurity concentration, and b is the blocking layer thickness. Only free electrons generated within the depletion region of a BIB detector can be collected by the positively biased contact. Electrons excited in the neutral region will recombine with a nearby ionized donor. In order to detect a large percentage of the incident photons it is necessary to achieve a value for the product of the linear absorption coefficient α and the depletion layer width w, $\alpha w \geq 2$. This, in turn, requires an appropriate depletion region width. As shown in Equation 1, the depletion region thickness is determined by the applied bias and the minority acceptor concentration within the device. The minimization of the compensating acceptor concentration is, therefore, of the greatest importance in achieving high quantum efficiency. For example, in order to detect 50% flux at 37 cm^{-1} (270 μm) for a GaAs BIB detector (neglecting surface reflection) with an active region majority doping of 6.7×10^{15} cm^{-3}, a 5 μm blocking layer, and an applied bias of 300 mV, it is necessary that the acceptor concentration be 1×10^{12} cm^{-3}. This corresponds to an acceptor to donor compensation ratio of 0.00014.

GaAs is an especially attractive material for BIB production because of its low donor electron binding energy (6 meV). This means that a bulk GaAs photoconductor would be sensitive to radiation well below 45.5 cm^{-1} (above 220 μm), the limit of detection by state of the art, stressed Ge:Ga photoconductors [14]. In an actual BIB detector, the response should extend to even longer wavelengths due to impurity band formation and broadening. This broadening is determined by two major factors. Impurity electron wavefunctions will increasingly overlap as the doping concentration is increased, and the aver-

age separation between impurity atoms decreases. Greater overlap causes an exchange interaction to occur between neighboring electrons, widening, and shifting the impurity band density of states closer to the conduction band. Dispersion of impurity energy levels also occurs due to the Stark broadening caused by the random electric fields associated with ionized donor and acceptor centers that have lost their electrons or holes due to compensation. In highly compensated samples, Stark broadening dominates at low doping, when impurity centers are widely spaced. Impurity banding dominates at higher doping concentrations. The concentration at which banding dominates over Stark broadening depends upon the compensation of the material [15]. For the case of Si:As BIB structures the BIB detector response is extended to 333 cm^{-1} (30 μm) while a more lightly doped bulk Si:As photoconductor responds up to only 400 cm^{-1} (25 μm).

A major difficulty for BIB detector production still exists, however, in obtaining low compensation GaAs [16]. The residual high acceptor concentration limits the depletion width in the active region of the device, leading to potentially low detection efficiency. We are currently researching the production of low compensation GaAs by Liquid Phase Epitaxy and other means to combat this problem.

For optimal BIB detector performance, the active region must be doped sufficiently high to obtain $\alpha w \geq 2$ and to widen the impurity band giving longer wavelength response. Too high of a doping concentration, however, will require greater cooling to reduce dark current generated by thermally excited carriers. At still higher doping, the impurity band will overlap with the conduction band, leading to a failure of the device. Here we present a study based on far-infrared absorption spectroscopy and variable temperature Hall effect

measurements to determine the optimal donor concentration for the production of n-type GaAs BIB detectors. Variable temperature Hall effect results demonstrate the transition to impurity band and hopping conductivity at low temperature. For the case of Si and Ge BIB detectors [11,17], the optimal active layer doping concentration was found to be roughly a factor of 10 lower than the concentration at the metal-insulator transition (MIT). Here the MIT has been determined by the Mott condition of Equation 2.

$$N^{\frac{1}{3}} a_{\mathrm{h}} = .25 \tag{2}$$

N is the shallow impurity concentration and a_{h} is the corresponding Bohr radius. Haegel [18] extrapolated this dependence to GaAs (N_{MIT}=2 $\times$ 10^{16} cm^{-3}) to predict an optimal BIB absorbing layer doping concentration close to 1 $\times$ 10^{15} cm^{-3}.

3 Experimental procedures

The far-infrared absorption spectrum for n-type GaAs as a function of doping concentration has been determined recently [19]. The absorption spectra for three n-type, Te doped GaAs Liquid Phase Epitaxial (LPE) films on semi-insulating GaAs substrates were recorded by Fourier Transform Infrared Spectrometry, as described in [19]. LPE is a desirable choice of growth technique for BIB detector production because it has been shown to produce GaAs films of extremely high purity and large thickness [20]. Tellurium was chosen as the dopant because of its low diffusivity in the solid phase and its relatively low vapor pressure compared to other n-type dopants such as sulfur. The low diffusivity is important so as to reduce the amount of Te that can diffuse

from the absorbing layer into the high purity blocking layer during growth. A broadening of the blocking layer-absorbing layer interface is expected to degrade the performance of the detector, and has been identified as an obstacle in the production of Ge BIB devices [17].

Hall effect and resistivity measurements on the GaAs samples were performed using In-Sn ohmic contacts that were annealed at 400°C for 10 minutes in nitrogen. A 3 kG magnetic field in alternating positive and negative configurations was used for the Hall effect portion of the measurement to eliminate the effect of magnetoresistance. The current used was lowered as the temperature fell in order to reduce resistive self-heating of the sample. For temperatures down to 4.2 K, the sample was attached to a copper cold finger that was cooled by a liquid helium flow system and contained within an evacuated cryostat. The temperature was maintained using a Lakeshore 331 temperature controller and heating resistor. Cooling below 4.2 K occurred inside a pumped liquid helium Dewar containing a ^{3}He absorption pump refrigerator.

4 Results and discussion

Absorption spectra taken from [19] are shown in Figure 2, at 2 cm^{-1} resolution and at temperature of 1.35 K. The photoconductivity spectrum of sample 191, which is of high purity (1×10^{14} cm^{-3}) is also shown. The relevant physical and electrical properties of these films are listed in Table 1.

[Fig. 2 about here.]

[Table 1 about here.]

From the photoconductivity result, the position of the 1s-2p transition, followed by thermal excitation to the conduction band is clearly seen at 35.5 cm^{-1}. The broader peak, centered at 49 cm^{-1} represents the 1s to continuum transition energy. The absorption spectra for the intentionally doped films, samples 286, 294, and 295, have their maxima at approximately 37 cm^{-1}. These spectra represent a combination of the two transitions observed by photoconductivity.

Far-infrared absorbance for the more highly doped films is considerably extended in comparison to the high purity photoconductivity result. As the doping concentration is increased the spectra broaden, reflecting the formation of impurity bands as the Te inter-impurity distance becomes smaller and their bound electron wavefunctions begin to overlap spatially, as described above. This effect can be seen in Figure 2, with the spectral response becoming broader as the concentration is increased. At the lowest doping concentration (sample 286), the absorption spectrum is relatively narrow. The spectra for the more heavily doped films extend over a wider spectral range. Impurity band formation has occurred to a large extent in these samples. There are no data near 70 cm^{-1} because this is the region of the first spectral minimum of the beamsplitter. The maximum absorption at 37 cm^{-1} corresponds to a wavelength of approximately 270 μm. This shows that a GaAs BIB detector will have a response at wavelengths significantly greater than the 220 μm limit characteristic of uniaxially stressed Ge:Ga photoconductors. The absorption coefficient falls to half of its peak value at 30 cm^{-1} (333 μm) for sample 286, and at 20 cm^{-1} (500 μm) for sample 295. This means that a GaAs BIB with an absorbing layer concentration of 6.7×10^{15} cm^{-3} should be sensitive to photons of wavelength as high as 500 μm.

Impurity band formation is also evident from the electronic transport measurements. Figure 3 displays the free electron concentration of the three samples as a function of inverse temperature. As the temperature is lowered the concentration of electrons in the conduction band will decrease as they freeze-out onto donor states. This is seen clearly in the free electron concentration of sample 286 in Figure 3. The slope of this exponentially decreasing carrier concentration region is related to the binding energy of the donor states that capture the electrons. For a highly compensated sample, the thermal activation energy is related to the slope of the freeze-out region ($slope = -\frac{E_{\rm th}}{k}$). $E_{\rm th}$ is the thermal activation energy for a bound donor electron and k is the Boltzmann constant. Using this relation, the thermal binding energies for samples 286 and 295 are determined to be 3 meV and 2.3 meV, respectively. The decrease in binding energy with increasing donor concentration reflects the broadening of isolated energy levels into a band with an upper edge closer to the conduction band edge. In the most lightly doped sample, 286 (1×10^{15} cm^{-3}), freeze-out of shallow donors continues down to a temperature of approximately 67 K. Below this point the impurity band is sufficiently populated with carriers such that electron hopping within the impurity band becomes the dominant conduction mechanism (instead of electron motion within the conduction band).

[Fig. 3 about here.]

The formation of impurity bands is further evident from temperature dependent resistivity measurements. Equation 3 relates the total resistivity of an n-type semiconductor to the sum of its three major components: electron travel within the conduction band (ρ_1), the upper Hubbard band (ρ_2), and

hopping between ionized donor atoms (ρ_3) [21].

$$\rho^{-1}(T) = \rho_1^{-1} e^{-\frac{\epsilon_1}{kT}} + \rho_2^{-1} e^{-\frac{\epsilon_2}{kT}} + \rho_3^{-1} e^{-\frac{\epsilon_3}{kT}} \tag{3}$$

Here the activation energy for each process is represented by $\epsilon_{\rm i}$, and $\rho_{\rm i}$ are experimentally determined pre-exponential factors. The transition to hopping conduction can be seen clearly by examining the temperature dependence of the resistivity as seen in Figure 3. A change in slope of the Arrenhius plot indicates a shift in the conduction mechanism to nearest neighbor hopping as the conduction band is depopulated of electrons. The dominance of hopping conductivity at very low temperatures indicates that there are not a large number of empty, conduction band like states mixed with the impurity band. The two bands are distinct. The activation energy for hopping conduction, ϵ_3, can be estimated from the slope of this curve at low temperatures. The activation energies, estimated from the data of Figure 4 are 0.27 meV for 1×10^{15} cm^{-3}, 0.018 meV for 6.7×10^{15} cm^{-3}, and 0.005 meV for 2×10^{15} cm^{-3}. The activation energies are strong functions of the impurity density as well as the compensation. This is because the nearest neighbor hopping process, which involves the absorption and re-emission of a phonon, requires an empty donor site to jump into. At low temperatures, the ionized donor concentration is very nearly equal to the concentration of compensating acceptors.

[Fig. 4 about here.]

The optimized dopant concentration for a BIB absorbing layer can be estimated based on the absorption spectra of Figure 2 and the electrical transport data of Figure 3 and Figure 4. The most lightly doped sample, 286 (1×10^{15} cm^{-3}), shows a sharp absorption cutoff near 26 cm^{-1}, a clear freeze-out region

in the variable temperature Hall effect results, and a characteristic hopping dependence of the resistivity. The well defined thermal activation energy for hopping and band conduction present in these samples, combined with well defined absorption maxima, suggests a clean separation of the impurity band states from the conduction band, as required for BIB operation. For sample 295 (6.7×10^{15} cm^{-3}), the separation of the conduction and impurity bands, although smaller than for sample 286, is still evident.

The absorption spectrum of the most heavily doped sample (294) extends to very low energy while its free electron concentration shows only very slight freeze-out behavior. Furthermore the resistivity of this sample is nearly constant with decreasing temperature, and the hopping activation energy is practically zero, indicating the dominance of conduction band conductivity over hopping in the impurity band. This suggests that sample 294 is approaching the metallic conduction regime. Since the freeze-out region of sample 294 is not well defined, a meaningful value of the activation energy cannot be extracted from the Hall effect data. It can therefore be inferred that the impurity band extends very close to the conduction band at the concentration of 2×10^{16} cm^{-3}, as predicted by the theory of Mott.

An active layer doped between the concentrations of 1×10^{15} cm^{-3} (sample 286) and 6.7×10^{15} cm^{-3} (sample 295), appears to be a good candidate for a GaAs BIB detector. In this range, a clear absorption maximum and shallow donor thermal activation energy exists. The linear absorption coefficients for this range vary between approximately 100 and 800 cm^{-1} for photons of 37 cm^{-1}, far greater than the values that could be achieved by a standard GaAs photoconductor. Below 1×10^{15} cm^{-3} doping concentration, the impurity to conduction band transition line width becomes narrow, limiting the optical

bandwidth of the detector. Furthermore, the absorption coefficient near 40 cm^{-1} of GaAs with doping less than 1×10^{15} cm^{-3} is relatively low, meaning that a BIB detector fabricated from such material would need a very thick depletion layer to have acceptable quantum efficiency. Above 6.7×10^{15} cm^{-3}, the impurity band to conduction band energy gap approaches zero. The absorbing layer doping concentration may have to be reduced below these values in case the LPE films are not homogeneously doped.

5 Conclusion

We have studied several LPE GaAs films with different doping concentrations using far-infrared absorption and variable temperature Hall effect and resistivity. The optimal majority doping concentration of the absorbing layer of a GaAs Blocked Impurity Band detector has been determined lie be between 1×10^{15} and 6.7×10^{15} cm^{-3}. While high compensation in the films must be reduced before a high sensitivity detector can be fabricated, we have shown that a BIB detector containing an infrared active region within this range would be highly absorbing for photons near 37 cm^{-1}. The absorption coefficient falls to 50% of its maximum value at 30 cm^{-1}, suggesting a GaAs BIB detector would have a wide spectral range of operation. It has been concluded that the impurity band for GaAs doped at these concentrations does not overlap with the conduction band edge, a necessity for proper BIB detector operation.

6 Acknowledgements

This work was supported by NASA Ames Research Center, Order No. A53228D through the U.S. Department of Energy under Contract No. DE-AC03-76SF00098.

References

[1] C.H. Townes, R. Genzel, Scientific American, April, 1990, pp. 46-55.

[2] J. T. Skidmore, J. Gildemeister, A. T. Lee, M. J. Myers, P. L. Richards, Applied Physics Letters, 82, 469 (2003).

[3] E.E. Haller, Infrared Physics and Technology, 35, 127 (1994).

[4] E. E Haller., W. L. Hansen, F. S. Goulding, IEEE Trans. Nucl. Sci. NS-22, 127 (1975).

[5] E. E. Haller, M. R. Hueschen, P. L. Richards, Applied Physics Letters, 34, 495 (1979).

[6] J. J. Hall, Phys. Rev. 128, 68 (1962).

[7] G. B. Heim, M. L. Henderson, K. I. Macfeely, T. J. Mcmahon, D. Michika, R. J. Pearson, G. H. Rieke, J. P. Schwenker, D.W. Strecker, C.L. Thompson, R.M. Warden, D. A. Wilson, E. T. Young, Proceedings of the SPIE, 3356, 985 (1998).

[8] http://sirtf.caltech.edu

[9] A. Poglitsch, C. Waelkens, N. Geis, Proceedings of the SPIE, 4013, 221 (2000).

[10] M. D. Petroff, M. G. Stapelbroek, US Patent no. 4568960.

[11] S. Pasquier, G. Sirmain, C. Meny, A. Murray, M. Griffin, P. Ade, L. Essalch, J. Galibert, J. Leotin, Proceedings of the SPIE, 2211, 634 (1994).

[12] J. Leotin, Infrared Physics and Technology, 40, 153 (1999).

[13] J. E. Van Cleve, T. L. Herter, R. Butturini, G. E. Gull, J. R. Houck, B. Pirger, J. Schoenwald, Proceedings of the SPIE, 2553, 513 (1995).

[14] R. Schnurr, C.L. Thompson, J.T. Davis, J.W. Beeman, J. Cadien, E.T. Young, E.E. Haller, G.H. Rieke, Proceedings of the SPIE, 3354, 322 (1998).

[15] D. M. Larsen, Phys. Rev. B 13, 1681 (1976).

[16] D. T. J. Hurle, J. Applied Physics, 85, 6957 (1999).

[17] J. Bandaru, J. W. Beeman, E. E. Haller, S. Samperi, N. M. Haegel, Infrared Physics and Technology, 43, 353 (2002).

[18] N. M. Haegel, Nuclear Inst. And Methods in Phys Research A, 377, 501 (1996).

[19] B. L. Cardozo, E. E. Haller, L. A. Reichertz, J. W. Beeman, Applied Physics Letters, 83, 3990 (2003).

[20] B. L. Cardozo, J. W. Beeman, E. E. Haller, Far-IR, Sub-mm and MM Detector Tech. Wkshp, Monterey, CA, www.sofia.usra.edu/det_workshop (2002).

[21] B.I. Shklovskii, A.L. Efros, Electronic Properties of Doped Semiconductors, Springer, Berlin, 1984.

List of Figures

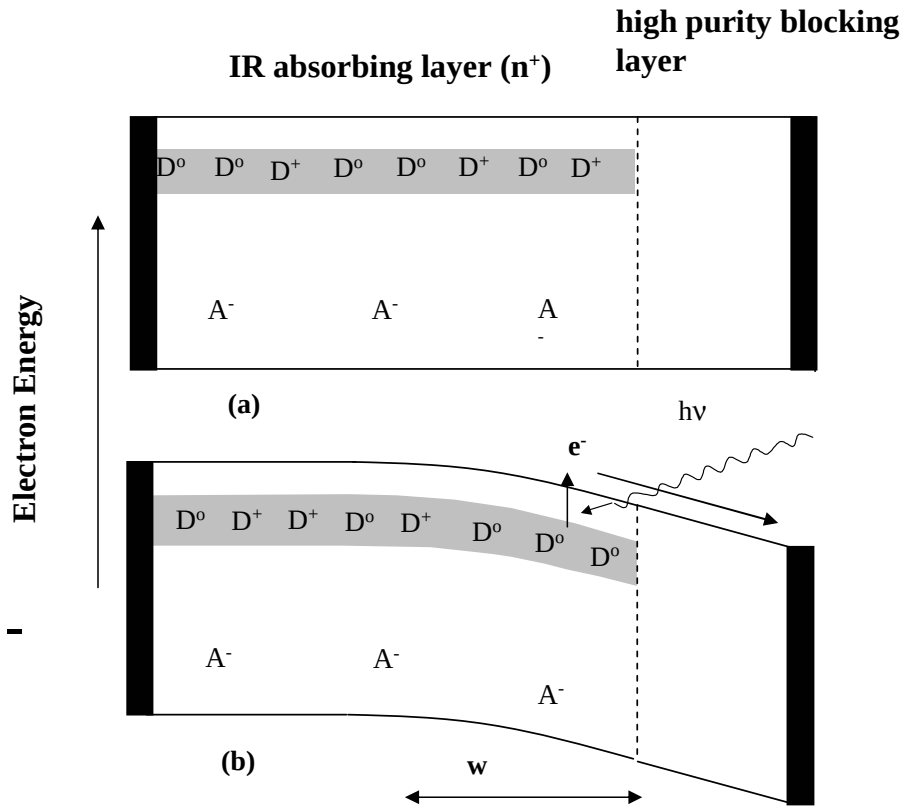

Fig. 1. Band diagram of a BIB detector a) unbiased, b) with an applied bias a depletion layer (w) forms.

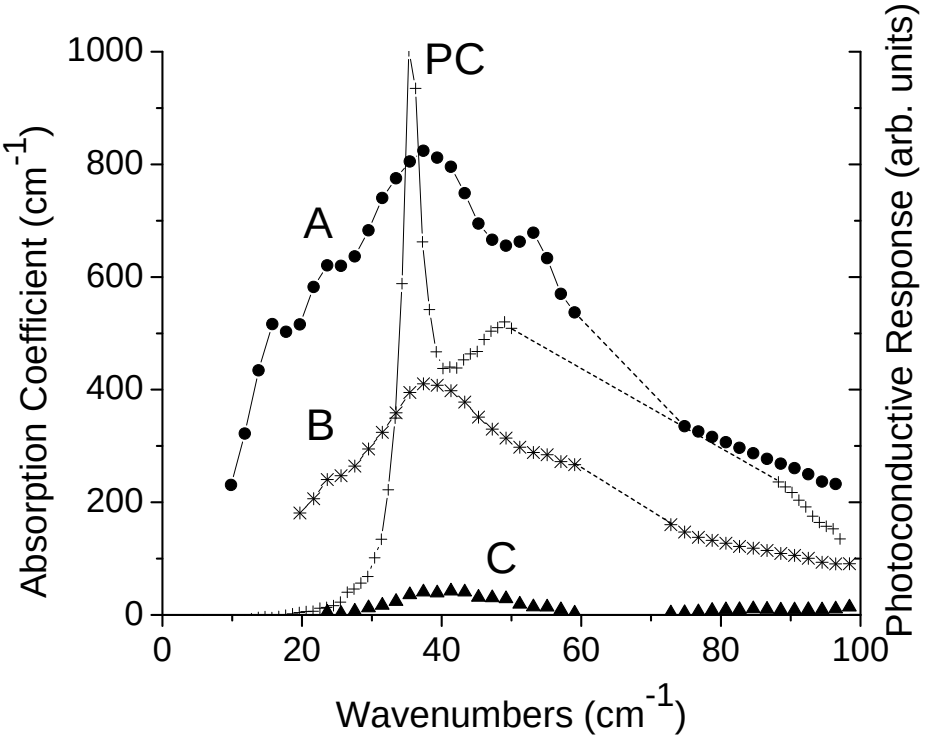

Fig. 2. GaAs absorption spectra show significant broadening compared to the photoconductivity spectrum for a high purity sample. Displayed are absorption spectra for: A) sample 294 (2.1×10^{16}), B) sample 295 (6.7×10^{15}), C) sample 286 (1.0×10^{15}), and the photoconductrivity spectrum for PC) sample 191 (1.0×10^{14}). The dashed lines near 68 cm^{-1} indicate loss of data due to a beamsplitter minimum. [19]

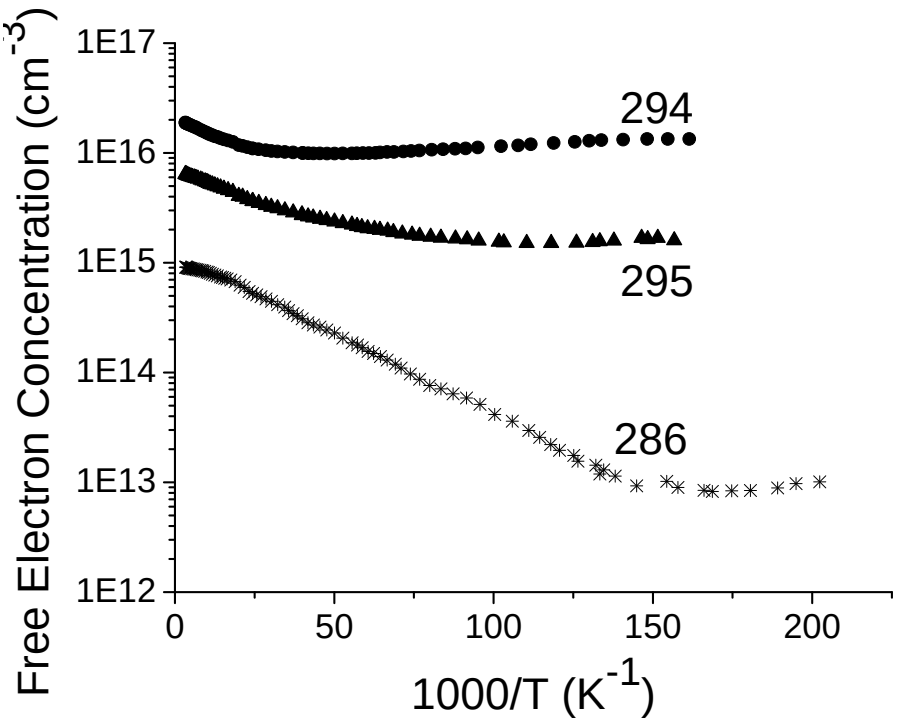

Fig. 3. Variable temperature Hall effect shows significantly more electron "freeze-out" behavior for sample 286 compared to samples 294 and 295.

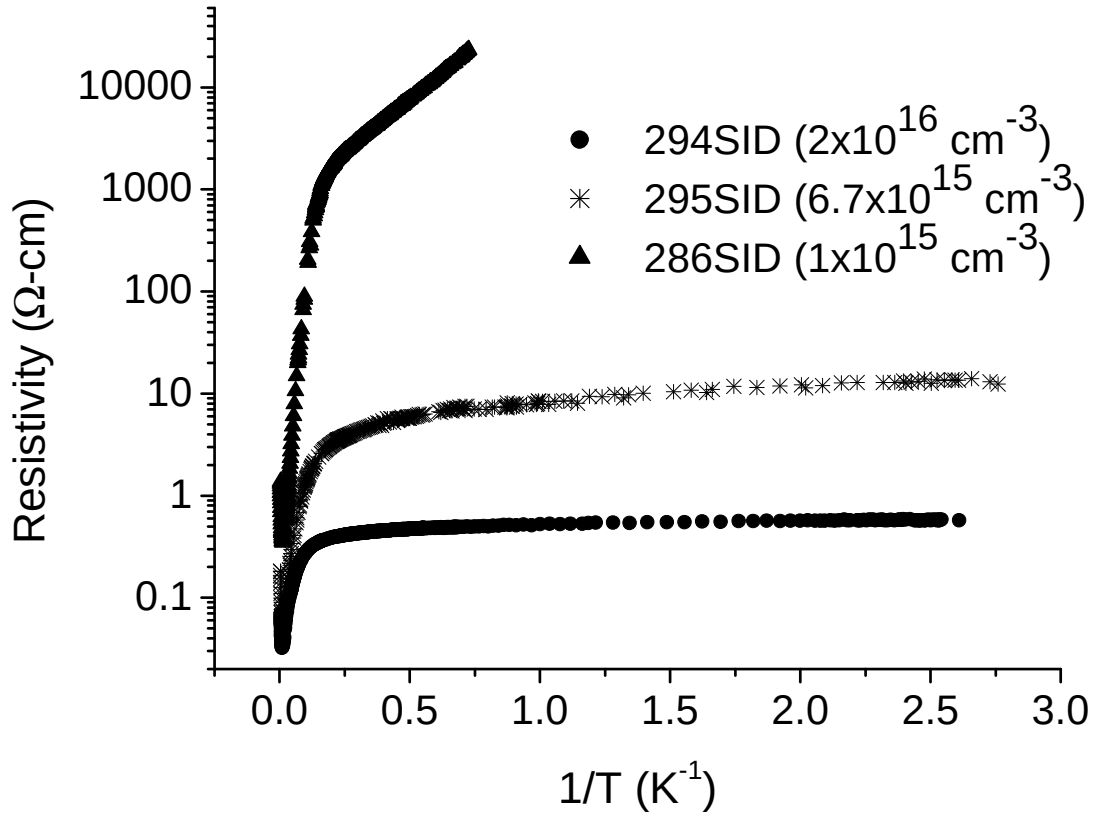

Fig. 4. Temperature dependence of the resistivity shows the dominance of hopping conduction at low temperatures for GaAs doped below 1×10^{16} cm^{-3}.

List of Tables

Table 1
Properties of sample used in absorption and carrier transport studies.

Sample	**Film thickness as measured (μm)**	$\mathbf{N_{300K}}$ **(cm^{-3})**	μ_{300K} **(cm^2/Vs)**
286	40	1.0×10^{15}	5680
294	66	2.0×10^{16}	4490
295	62	6.7×10^{15}	5280
191	100	1.0×10^{14}	7440